

## *Energy Losses of Q-balls.*

*D. Bakari<sup>a,b</sup>, H. Dekhissi<sup>a,b</sup>, J.Derkaoui<sup>a,b</sup>, G. Giacomelli<sup>a</sup>,  
G. Mandrioli<sup>a</sup>, M. Ouchrif<sup>a,b</sup>, L. Patrizii<sup>a</sup>, V. Popa<sup>a,c</sup>.*

<sup>a</sup>Dipartimento di Fisica dell' Università di Bologna, INFN sezione di  
Bologna, Italy.

<sup>b</sup> Faculté des sciences (LPTP), Université Mohamed 1<sup>er</sup>, Oujda, Morocco.

<sup>c</sup> Institute for Space Sciences, Bucharest, Romania.

### *Abstract*

After a short review of Q-balls properties, in this paper we discuss their interaction with matter, and their energy losses in the earth, for a large range of velocities. These calculations are used to compute the fractional angular acceptance of a detector at Gran Sasso Laboratory. Furthermore we computed the light yield in liquid scintillators, the ionization in streamer tubes and the Restricted Energy Loss in the CR39 nuclear track detector.

*Submitted to Astroparticle Physics*

# 1 Introduction

Dark Matter (DM) is one of the intriguing problems in particle physics and cosmology. Several types of stable (or quasi stable) particles have been proposed as candidates for the cold DM. Among these candidates one has the nuclearites (strange quark matter), which are agglomerates of quarks  $u, d$  and  $s$  [1]. Another example of cold DM candidate, coming from theories beyond the standard Model of particle physics, is the lightest supersymmetric particle (LSP) [2].

In theories where scalar fields carry a conserved global quantum number,  $Q$ , there may exist non-topological solitons which are stabilized by global charge conservation. They act like homogenous balls of matter, with  $Q$  playing the role of the quantum number; Coleman called this type of matter *Q-balls* [3].

The conditions for the existence of absolutely stable Q-balls are satisfied in supersymmetric theories with low energy supersymmetry breaking<sup>1</sup> [4]. The role of conserved quantum number is played by the baryon number (The same reasoning applies to the lepton number for the sleptonic Q-balls). Q-balls can be considered like coherent states of squarks, sleptons and Higgs fields. Under certain assumptions about the internal self interaction of these particles and fields the Q-balls could be absolutely stable [5].

In this note we summarize the main physical and astrophysical properties of Q-balls, their interactions with matter, their energy losses in detectors, and the possibility of traversing the earth to reach any detector at the underground Gran Sasso Laboratory (Italy), for example MACRO [6]. We neglect the possibility of: (i) electromagnetic radiation emitted by Q-balls of high  $\beta$ , (ii) strong interactions of Q-balls in the upper atmosphere capable of destroying the Q-ball, and (iii) the possibility that neutral Q-balls (SENS) may become charged (SECS) and viceversa [2].

---

<sup>1</sup>According to ref. [5], abelian non-topological solitons with baryon and/or lepton quantum numbers naturally appear in the spectrum of the Minimal Supersymmetric Standard Model.

## 2 Properties of Q-balls

Q-balls could have been produced in the Early Universe, and may contribute to the cold DM. Several mechanisms could have lead to the formation of Q-balls in the Early Universe. They may have originated in the course of a phase transition, which is sometimes called “solitogenesis”, or they could have been produced via fusion processes, reminiscent of the Big Bang nucleosynthesis, which have been called “ solitosynthesis”; small Q-balls could be pair-produced in very high energy collisions (at high temperatures) [4].

The astrophysical consequences of Q-balls in many ways resemble those of strange quark matter, nuclearites.

One of the peculiarities of Q-balls is that their mass grows as  $Q^{3/4}$ , while for nuclearites the mass grows linearly with the baryon number [1].

In the squark bag there is an almost uniform potential  $U(\phi)$ , which may be taken as  $U(\phi) \sim M_S^4 = \text{constant}$  in SUSY theories with low energy supersymmetry breaking [8]. For large scalar  $\phi$ , the mass  $M_Q$  and radius  $R_Q$  of Q-balls with baryon number  $Q$  are given by [8]:

$$M_Q = \frac{4\pi\sqrt{2}}{3} M_S Q^{3/4} \simeq 5924 \left( \frac{M_S}{1 \text{ TeV}} \right) Q^{3/4} \quad (GeV)$$

$$\simeq 1.2 \times 10^{-20} \left( \frac{M_S}{1 \text{ TeV}} \right) Q^{3/4} \quad (g) \quad (1)$$

$$R_Q = \frac{1}{\sqrt{2}} M_S^{-1} Q^{1/4} \simeq 1.4 \times 10^{-17} \left( \frac{1 \text{ TeV}}{M_S} \right) Q^{1/4} \quad (cm) \quad (2)$$

The parameter  $M_S$  is the energy scale of the SUSY breaking symmetry. The first parts of formulae (1), (2) are in  $\hbar = c = 1$  units; the last parts are in cgs units. A stability condition of the stable Q-ball mass  $M_Q$  is related to the proton mass  $M_p$  by

$$M_Q < Q M_p \quad (3)$$

From Eq. 1 and Eq. 3 one has the stability constraint

$$Q > \frac{M_Q}{M_p} = 1.6 \times 10^{15} \left( \frac{M_S}{1 \text{ TeV}} \right)^4 \quad (4)$$

In Fig. 1 the allowed region for stable Q-balls is indicated as a shaded region in the plane  $(Q, M_S)$ . The dashed lines indicate the Q-ball number as function of  $M_S$  assuming different Q-ball masses  $M_Q$ ; the dotted lines represent  $Q(M_S)$  for different Q-balls radii  $(R)$ .

Relic Q-balls are expected to concentrate in galactic halos and to move at the typical galactic velocity  $v = \beta c \simeq 10^{-3}c$ . Assuming that Q-balls constitute the cold galactic dark matter with  $\rho_{DM} \sim 0.3 \text{ GeV}/\text{cm}^3$ , their number density is [8]

$$\begin{aligned} N_Q &\sim \frac{\rho_{DM}}{M_Q} \sim \rho_{DM} \left( \frac{3}{4\pi\sqrt{2}} \right) Q^{-3/4} M_S^{-1} \\ &\sim 5 \times 10^{-5} Q^{-3/4} \left( \frac{1 \text{ TeV}}{M_S} \right) \text{ cm}^{-3} \end{aligned} \quad (5)$$

The corresponding flux is [8]

$$\begin{aligned} \phi &\simeq \frac{1}{4\pi} N_Q v = \frac{\rho_{DM} v}{4\pi M_Q} \\ &\simeq \frac{1}{4\pi} \rho_{DM} \left( \frac{4\pi\sqrt{2}}{3} \right)^{-1} Q^{-3/4} M_S^{-1} v \\ &\simeq 10^2 Q^{-3/4} \left( \frac{M_S}{1 \text{ TeV}} \right)^{-1} v \quad (\text{cm}^{-2} \text{s}^{-1} \text{sr}^{-1}) \end{aligned} \quad (6)$$

In Fig. 2 we present the dependence of the Q-ball radius  $R_Q$  from its mass  $M_Q$  for two values of the  $M_S$  parameter. Q-balls with  $M_Q \leq 10^8 \text{ GeV}$  are unstable; Q-balls with  $M_Q \geq 10^{25} \text{ GeV}$  should be very rare.

In Fig. 3 we present the Q-ball flux versus Q-ball mass assuming that the density of the DM is  $\rho = 0.3 \text{ GeV}/\text{cm}^3$ , that all of it is in the form of Q-balls and that  $\beta \sim 10^{-3}$ . If Q-balls are part of the DM, their flux cannot be higher than that of the top dotted-dashed line in Fig. 3.

When traversing normal matter, Q-balls could form some sort of bound states with quarks (which remain in their outer layers), acquiring a positive electric charge. Electrons around the Q-ball can be captured through the reaction  $ue \rightarrow d\nu_e$  or could leave the Q-ball charged if the rate of this reaction is small, otherwise they would neutralise it [8].

Q-balls can be classified in two classes: **SECS** (Supersymmetric Electrically Charged Solitons) and **SENS** (Supersymmetric Electrically

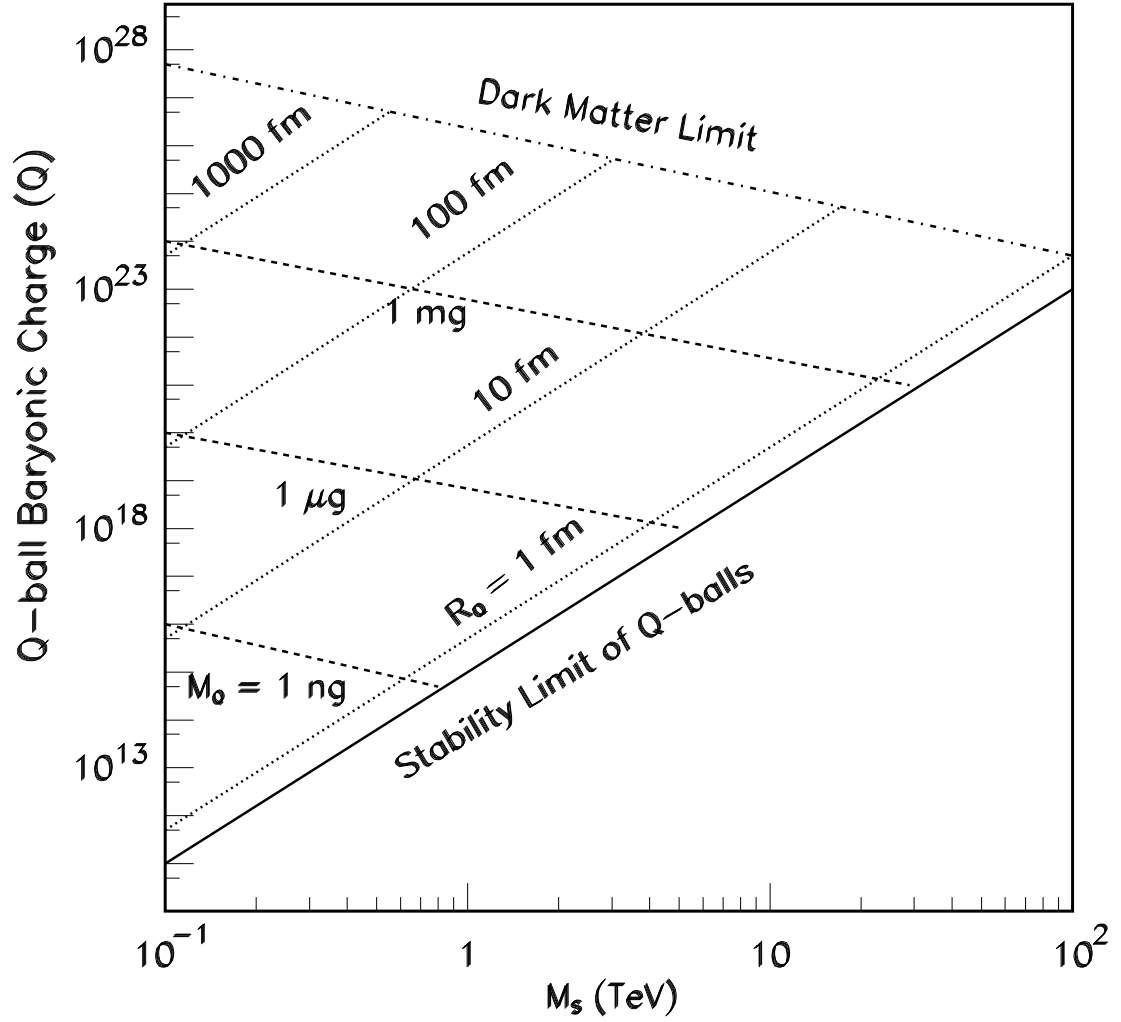


Figure 1: Q-ball number versus the supersymmetry energy scale  $M_S$  for Q-balls. The allowed region is delimited from below by the Q-ball stability limit (Eq. 4); assuming that they are part of the galactic DM and have  $\beta \sim 10^{-3}$ , they are limited from above by the dashed-dotted line. The dashed lines are  $Q = Q(M_s)$  for different Q-balls masses  $M_Q$ ; the dotted lines are  $Q = Q(M_s)$  for different Q-balls radii  $R_Q$ .

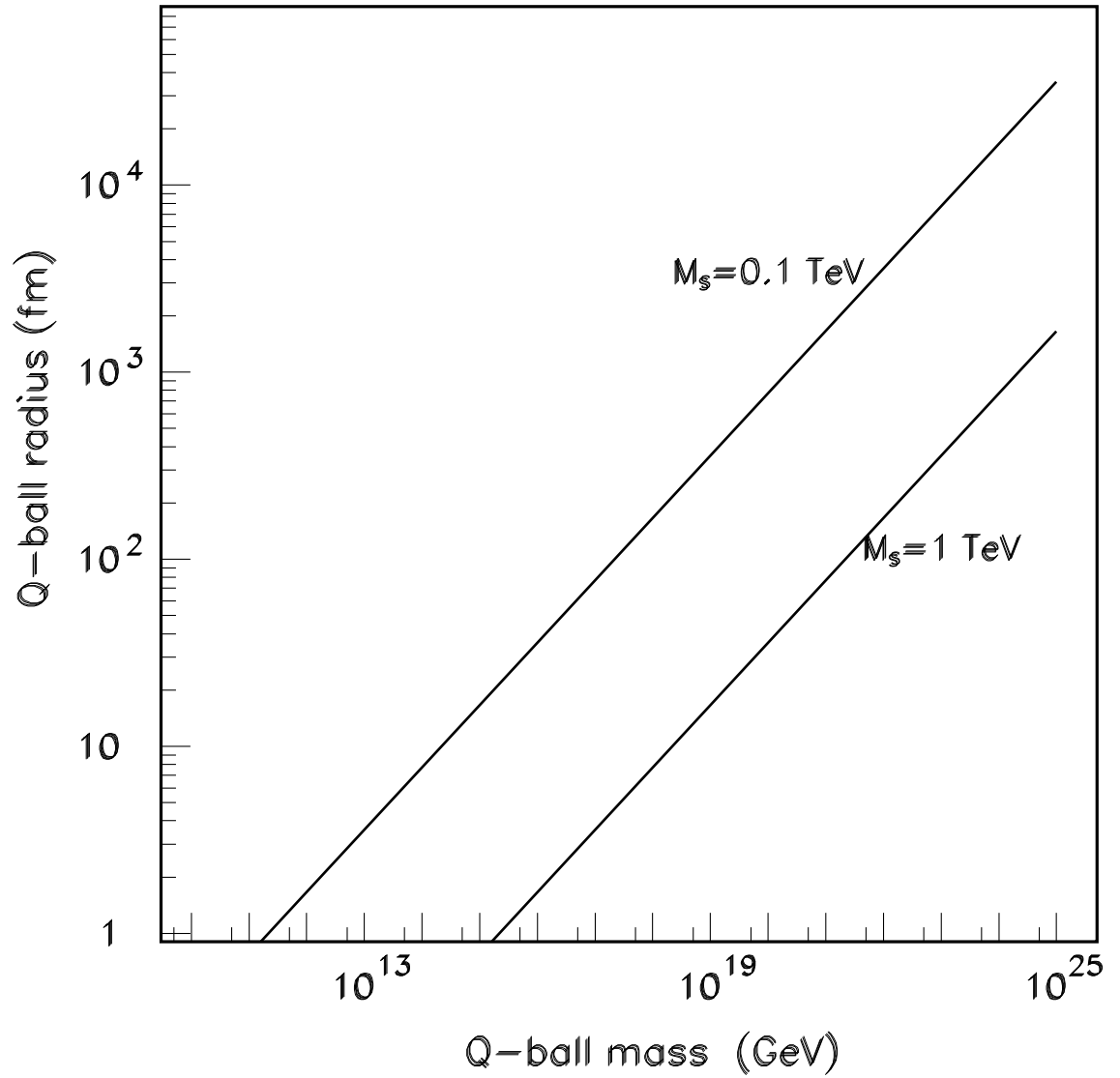


Figure 2: Dependence of the Q-ball radius  $R_Q$  from its mass  $M_Q$  for two values of the  $M_S$  parameter. Q-balls with  $M_Q \leq 10^8$  GeV/ $c^2$  are unstable; Q-balls with  $M_Q \geq 10^{25}$  GeV/ $c^2$  should be very rare.

Neutral Solitons). The interactions of Q-balls with matter and their detection differ drastically for SECS or SENS [2].

### 3 Interaction with matter

Q-balls could have velocities typical of objects bound to the galaxy,  $10^{-4} < \beta < 10^{-2}$ . Thus we do not expect relativistic Q-balls. For reasons of completeness we estimate the energy losses even for relativistic Q-balls, which we indicate as dotted lines in Figs. 3, 4.

#### 3.1 Interactions with matter of Q-balls type SECS

SECS are Q-balls with a net positive electric charge which tends to be mainly in the outer layer. The charge of SECS originates from the unequal rates of absorption in the condensate. The positive electric charge could be of one unit up to several tens. This positive electric charge may be neutralized by a surrounding cloud of electrons.

For small size Q-balls the positive charge interacts with matter (electrons and nuclei) via elastic or quasi elastic collisions. The cross section is similar to the Bohr cross section of hydrogenoid atoms [5]:

$$\sigma = \pi a_0^2 \sim 10^{-16} \text{ cm}^2 \quad (7)$$

where  $a_0$  is the Bohr radius. The formula is valid for  $R_Q \leq a_0$ , which happens for  $Q \leq 2.7 \times \left(\frac{M_S}{1 \text{ TeV}}\right)^4$ . For  $Q \geq 2.7 \times \left(\frac{M_S}{1 \text{ TeV}}\right)^4$  the Q-ball radius is larger than  $a_0$ , and it increases with the Q-ball mass. Thus electrons could find themselves inside the Q-ball, for large Q-ball masses. One could assume that in such conditions the electronic capture is favoured and thus the SECS tend to become SENS.

The main energy losses [6] of SECS passing through matter with velocities in the range  $10^{-4} < \beta < 10^{-2}$  are due to the interaction of the SECS positive charge: (i) with the nuclei (nuclear contribution), and (ii) with the electrons of the traversed medium (electronic contribution). The total energy loss is the sum of the two contributions.

SECS could cause the catalysis of proton decay, but only in the case for

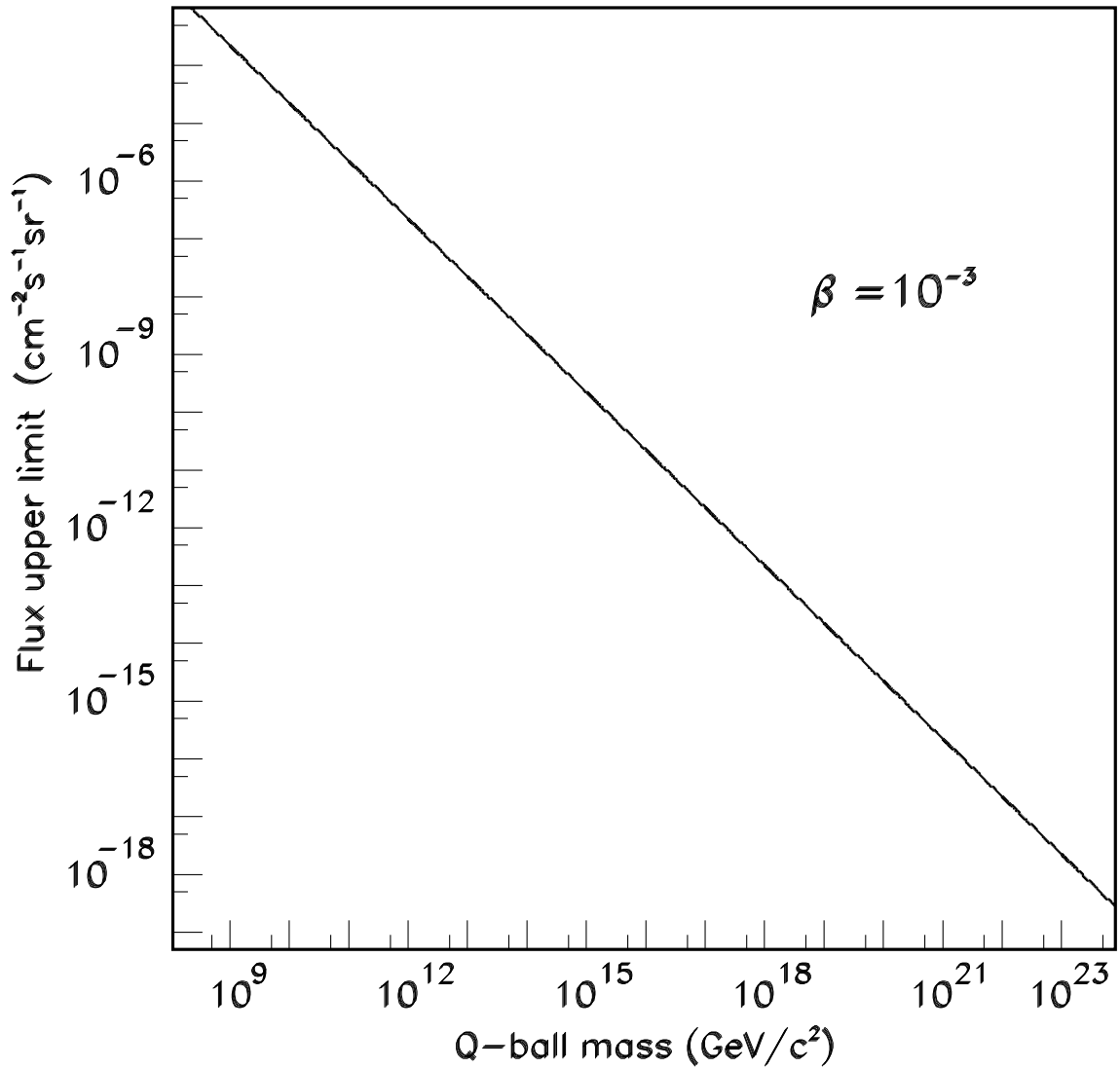


Figure 3: Q-ball flux in the cosmic radiation versus Q-ball mass assuming that the density of DM is  $\rho = 0.3 \text{ GeV}/\text{cm}^3$ , that it is all in the form of Q-balls and that  $\beta \sim 10^{-3}$ . Clearly if Q-balls are 0.1% of the total DM, the Q-ball flux is smaller by a factor of  $10^3$ .



$$R_Q \geq \frac{2Z_Q e^2}{m_e v^2} \quad (8)$$

where  $v$  and  $Z_Q$  are respectively the velocity and the positive electric charge of the SECS,  $m_e$  is the electron mass [9] (see Fig. 2). For  $\beta = 10^{-3}$ ,  $Z_Q = 1$  this corresponds to radii larger than  $10^3$  fm and masses larger than 1 mg, which are very large values. The probability of catalysis by large mass SECS is reduced by the presence of their electric charge.

**Electronic losses of SECS:** The electronic contribution to the energy loss of SECS may be computed with the following formula [6]

$$\frac{dE}{dx} = \frac{8\pi a_0 e^2 \beta}{\alpha} \frac{Z_Q^{7/6} N_e}{(Z_Q^{2/3} + Z^{2/3})^{3/2}} \quad \text{for } Z_Q \geq 1 \quad (9)$$

where  $\alpha$  is the fine structure constant,  $\beta = v/c$ ,  $Z_Q$  is the positive charge of SECS,  $Z$  is the atomic number of the medium and  $N_e$  is the density of electrons in the medium. Electronic losses dominate for  $\beta > 10^{-4}$  (see Figs 3 and 4 for the case of the  $dE/dx$  in the Earth).

**Nuclear losses of SECS:** The nuclear contribution to the energy loss of SECS is due to the interaction of the SECS positive charge with the nuclei of the medium and it is given by [6]

$$\frac{dE}{dx} = \frac{\pi a^2 \gamma N E}{\epsilon} S_n(\epsilon) \quad (10)$$

where

$$S_n(\epsilon) \simeq \frac{0.56 \ln(1.2\epsilon)}{1.2\epsilon - (1.2\epsilon)^{-0.63}}, \quad \epsilon = \frac{a M E}{Z_Q Z e^2 M_Q} \quad (11)$$

and

$$a = \frac{0.885 a_0}{(\sqrt{Z_Q} + \sqrt{Z})^{2/3}}, \quad \gamma = \frac{4M}{M_Q} \quad (12)$$

$M_Q$  is the mass of the incident Q-ball;  $M$  is the mass of the target nucleus;  $Z_Q e$  and  $Z e$  are their electric charges;  $a$  is the screening radius and  $a_0$  is the Bohr radius; we assume that  $M_Q \gg M$ . Nuclear losses dominates for  $\beta \leq 10^{-4}$  (see Figs. 3 and 4).

**The energy losses of SECS in the Earth mantle and Earth core:** The energy losses of SECS in the Earth mantle and Earth core have been

computed for different  $\beta$ -regions and for different charges of the Q-ball core, employing the same general procedures used for computing the energy losses in the Earth of magnetic monopoles and of nuclearites [6]. The results of the calculations are presented in Figs. 3 and 4; the dashed lines indicate interpolations.

Considering the energy losses discussed above, we have computed for a specific velocity ( $v = 250 \text{ km/s}$ ) the angular acceptance ( $\Omega/4\pi$ ) of the MACRO detector (located at an average depth of 3700 m.w.e.) for SECS (with  $Z_Q = 1$ ), see Fig. 5. Notice that for  $M_Q \geq 10^{12} \text{ GeV}$  the angular acceptance is  $2\pi$  (corresponding to SECS coming only from above), while for  $M_Q \geq 10^{22} \text{ GeV}$  the geometrical acceptance is  $4\pi$ .

Fig. 6 shows the accessible regions in the plane ( $M, \beta$ ) for Q-balls type SECS with  $Z_Q = 1$ , coming from above (to the right of the dashed curve) and from below (to the right of the solid line), respectively. Notice that SECS coming from above (below) may reach MACRO only if they have masses larger than  $\sim 10^{13} \text{ GeV}$  ( $\sim 10^{18} \text{ GeV}$ ).

### 3.2 Interactions of Q-balls type SENS

The Q-ball interior of SENS is characterized by a large Vacuum Expectation Value (VEV) of squarks, and may be of sleptons and Higgs fields <sup>2</sup> [5]. The  $SU(3)_c$  symmetry is broken and deconfinement takes place inside the Q-ball.

If a nucleon enters the region of deconfinement, it dissociates into three quarks, some of which may then become absorbed in the supersymmetric condensate [7-8]. The nucleon enters the  $\tilde{q}$  condensate and giving rise to processes like

$$qq \rightarrow \tilde{q}\tilde{q} \tag{13}$$

In practice one has

$$(Q) + \text{Nucleon} \rightarrow (Q + 1) + \text{pions} \tag{14}$$

and less probably,

$$(Q) + \text{Nucleon} \rightarrow (Q + 1) + \text{kaons} \tag{15}$$

---

<sup>2</sup>Also SECS have in their interior a large VEV of squarks, sleptons and Higgs fields; in addition they have a positive electric charge, and thus a coulomb potential which reduces the possibility of the catalysis of proton decay.

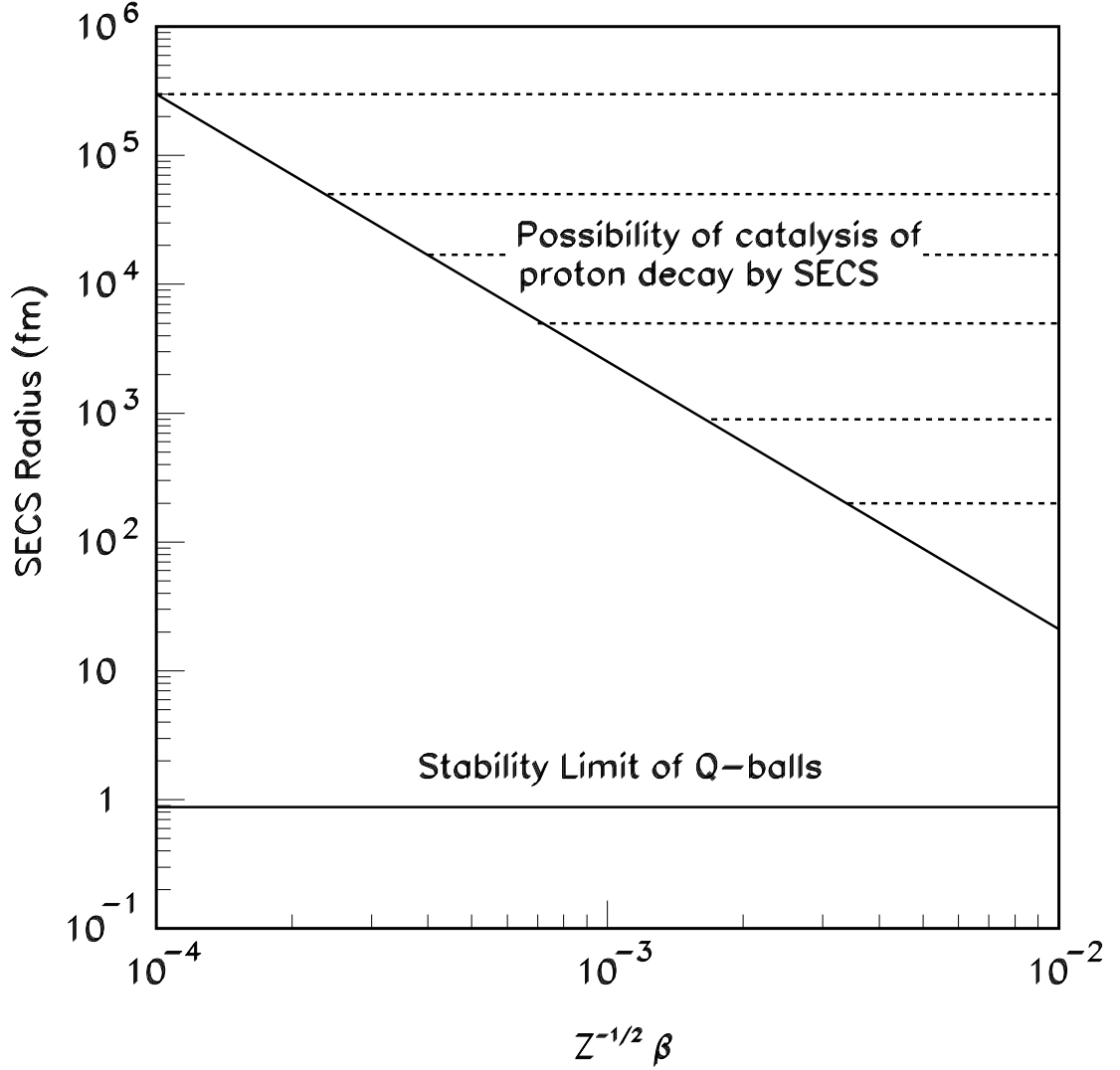


Figure 4: For SECS: Q-ball radius  $R_Q$  versus  $Z^{-1/2}\beta$ , where  $Z_Q$  is the positive net charge of the Q-ball core,  $\beta = v/c$ . The lower line indicates the stability limit of Q-balls corresponding approximately to a Q-ball mass of  $\sim 10^8$  GeV. The upper solid line gives the minimal Q-ball radii of SECS that could catalyse proton decay, Eq. 8.

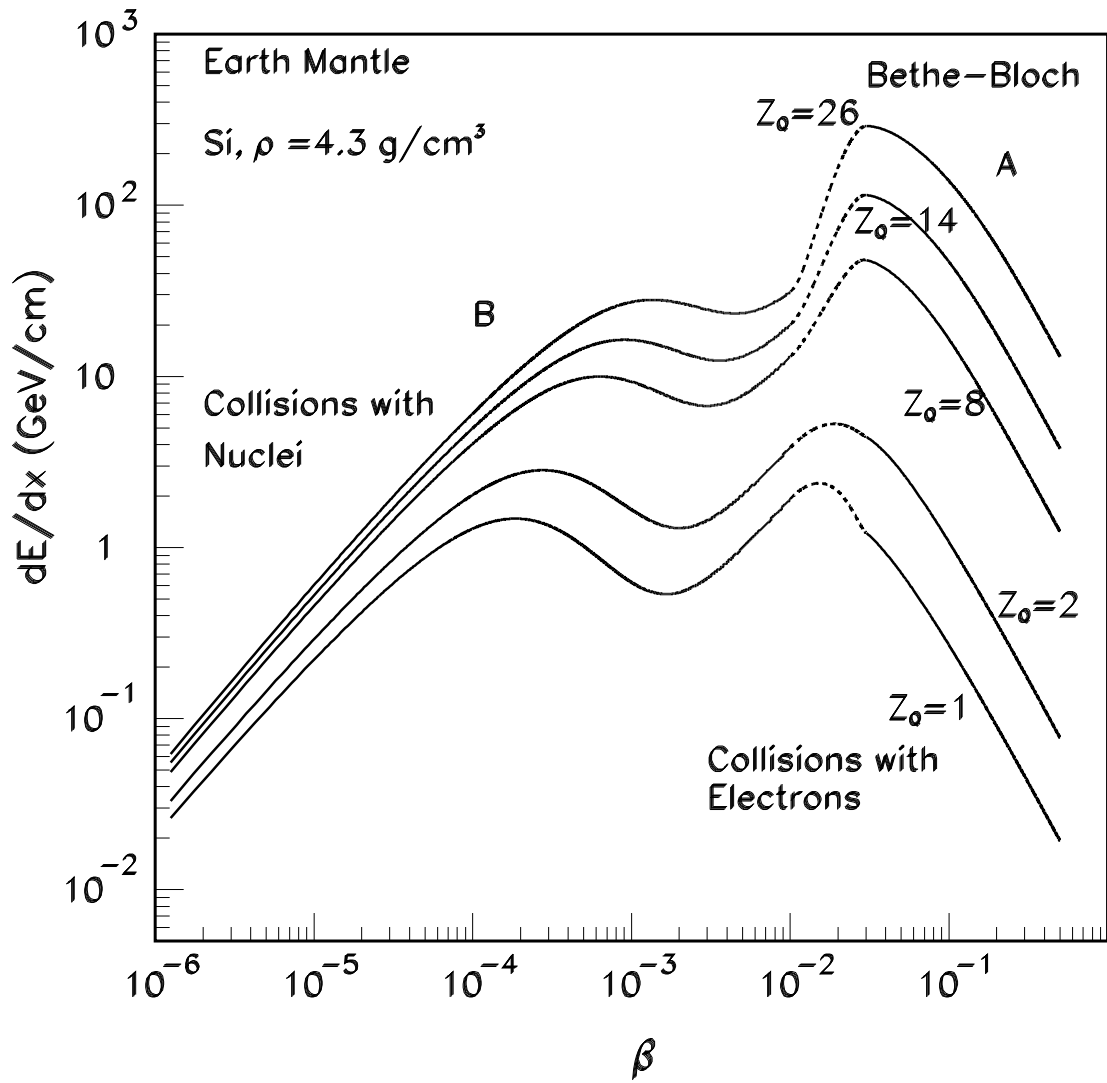


Figure 5: Energy losses of SECS versus  $\beta$  in the Earth mantle;  $Z_Q$  is the electric charge of the Q-ball. The possibility of the emission of electromagnetic radiation at high  $\beta \simeq 1$  was not considered.

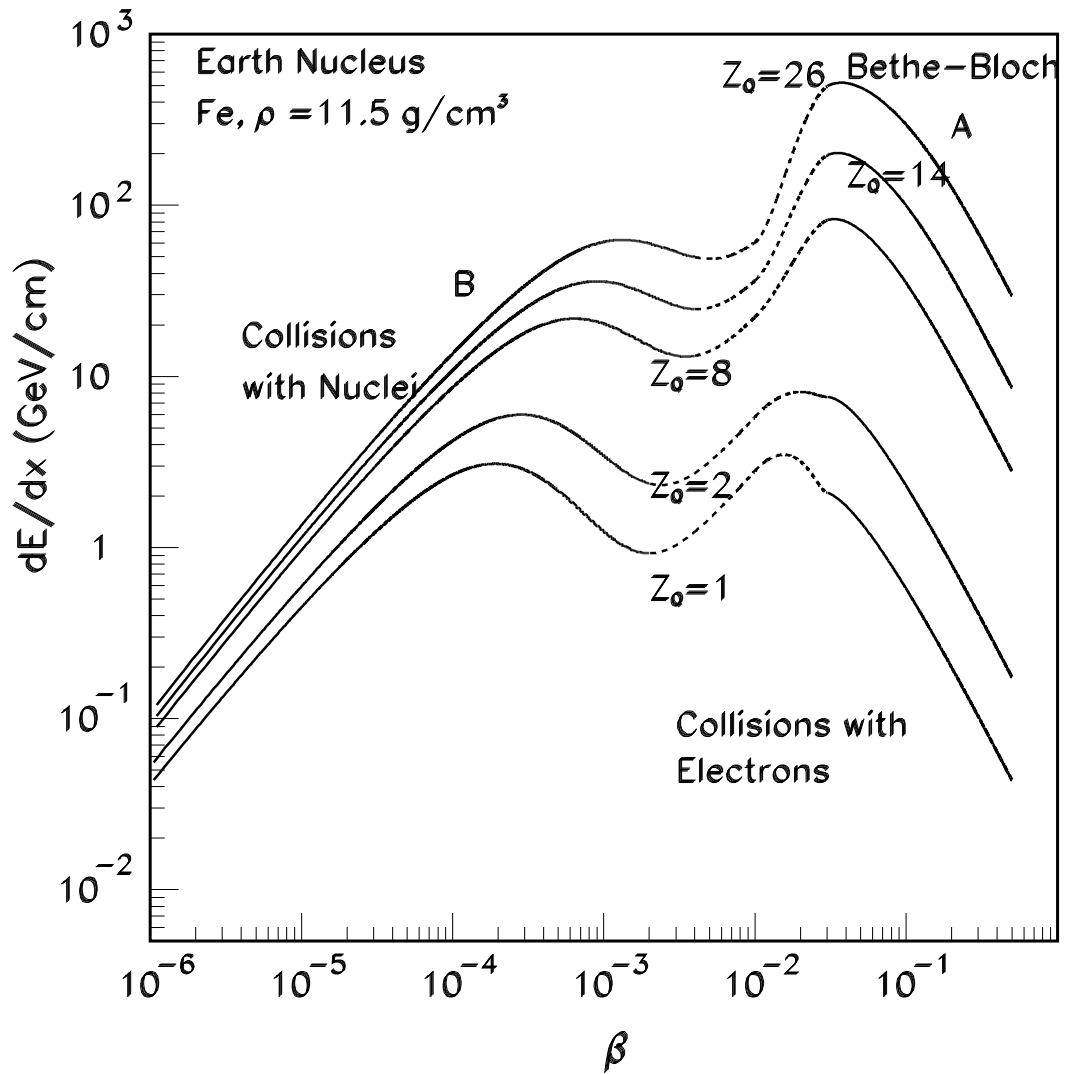


Figure 6: Energy losses of SECS versus  $\beta$  in the Earth core.  $Z_Q$  is the electric charge of the Q-ball. The possibility of emission of electromagnetic radiation at high  $\beta \simeq 1$  was not considered.

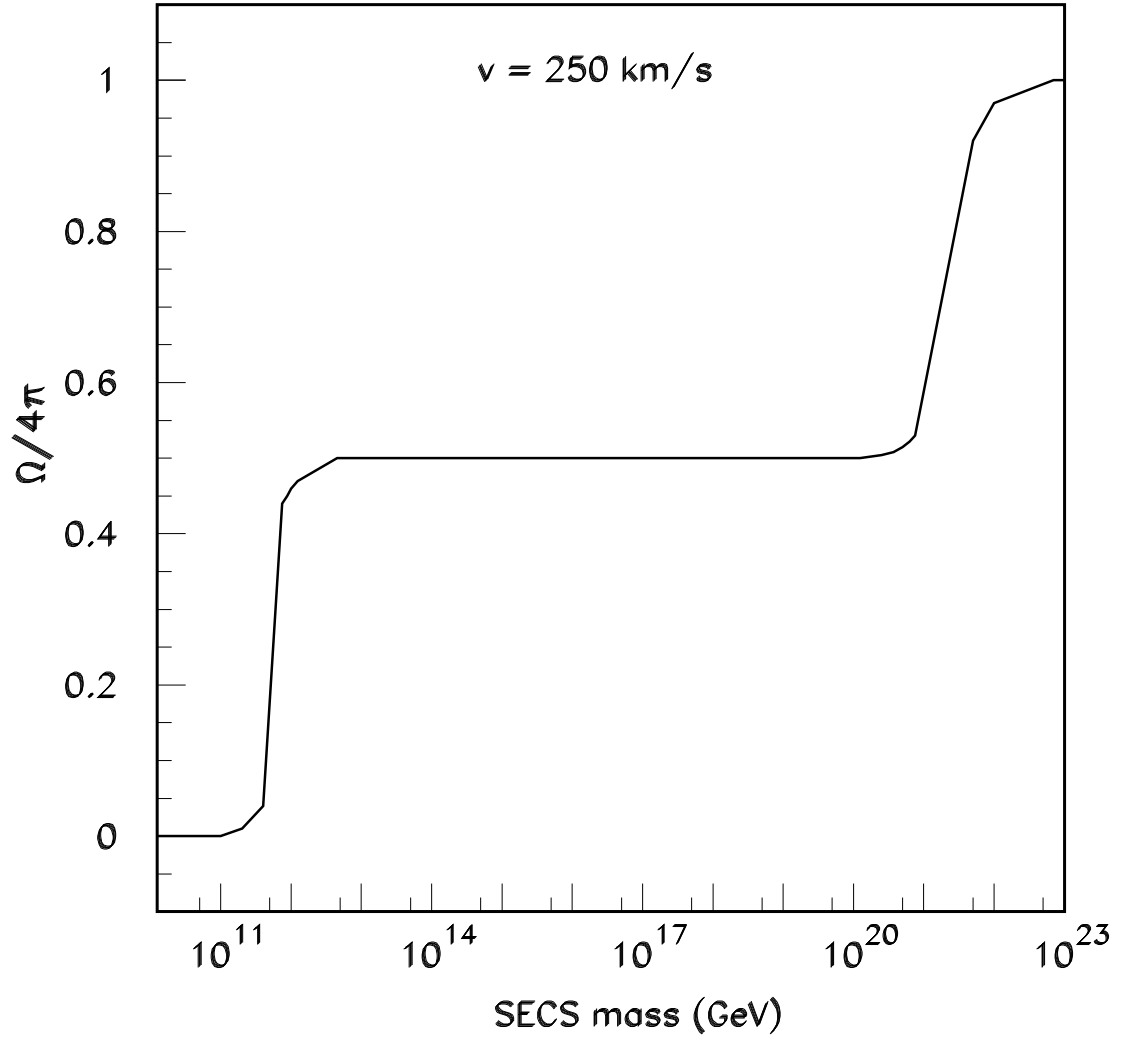


Figure 7: Angular acceptance of the MACRO detector for Q-balls type SECS with electric charge  $Z_Q = 1$  and incoming velocity  $v = 250 \text{ km/s}$ , as function of the Q-ball mass  $M_Q$ . For  $M_Q \geq 10^{12} \text{ GeV}$  the acceptance is  $2\pi$  (only SECS from above), while for  $M_Q \geq 10^{22} \text{ GeV}$  it is  $4\pi$

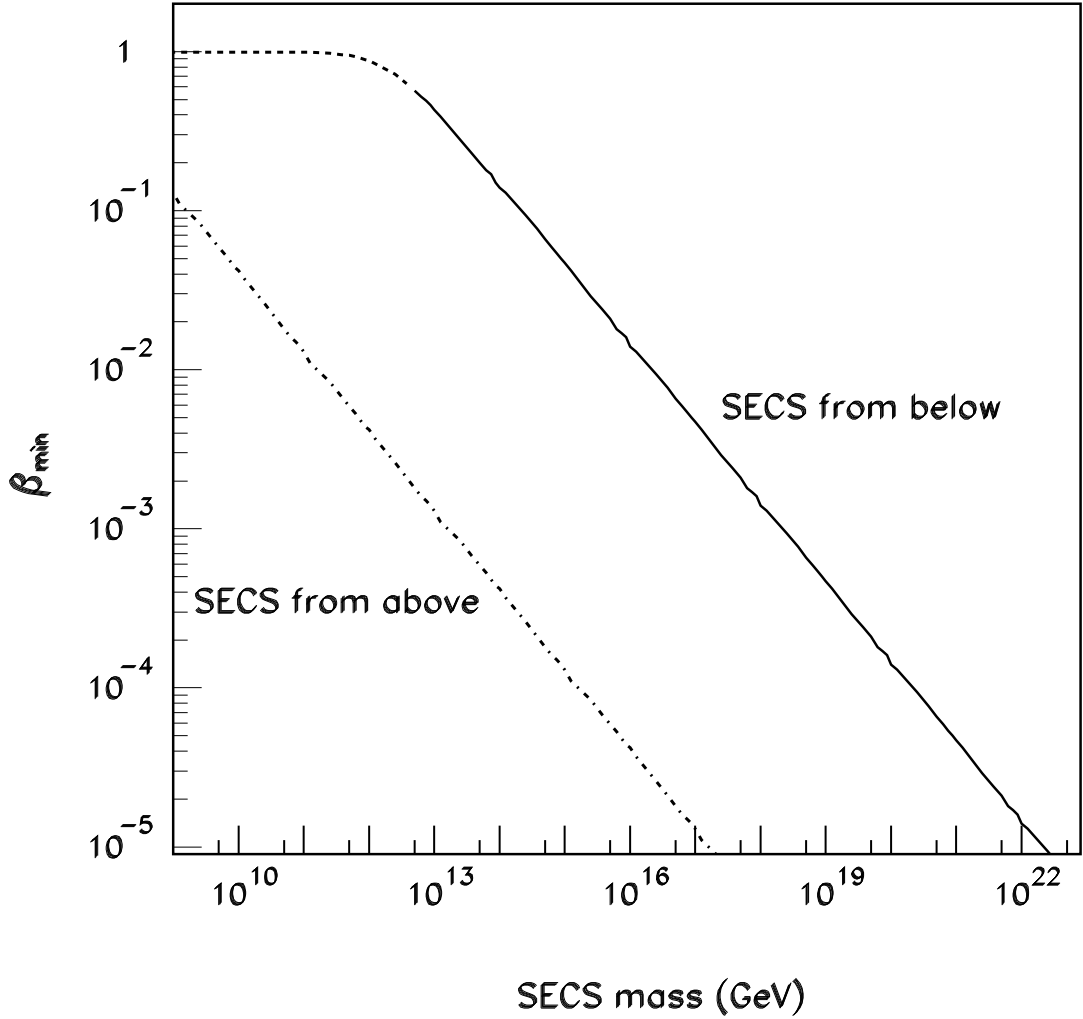


Figure 8: Accessible region in the plane (mass,  $\beta$ ) of SECS with electric charge  $Z_Q = 1$ . The solid (dotted-dashed) line, gives the minimum value of  $\beta$  ( $\beta_{min}$ ) that a SECS could have to reach the MACRO detector from above (below); the accessible region to the upper right of the two curves. The dashed line is an extrapolation of the solid line to very large values of  $\beta$ .

The pions carry the electric charge of absorbed nucleon (for example  $\pi^+\pi^0$ ).

If it is assumed that the energy released in (14) and (15) is the same as in typical hadronic processes (about 1 GeV per nucleon), this energy is carried by 2 or 3 pions (or kaons). The cross section for reactions (13) and (14) are determined by the Q-ball radius  $R_Q$  [5]

$$\sigma = \pi R_Q^2 = \frac{16\pi^2}{9} M_Q^{-2} Q^2 \sim 6 \times 10^{-34} Q^{1/2} \left( \frac{1 \text{ TeV}}{M_S} \right)^2 \text{ cm}^2 \quad (16)$$

The corresponding mean free path  $\lambda$  is

$$\lambda = \frac{1}{\sigma n} \quad (17)$$

where  $n$  is the number of atoms per  $\text{cm}^3$  in the traversed material. According to refs. [6-8] the energy loss of SENS moving with velocities in the range  $10^{-4} < \beta < 10^{-2}$  is constant and is given by

$$\frac{dE}{dx} \sim \frac{\zeta}{\lambda} = \sigma n \zeta \sim 6 \times 10^{-34} Q^{1/2} n \zeta \quad (18)$$

where  $\zeta = 1 (\rho/1g \text{ cm}^{-3}) \text{ GeV}$  is the energy released in one reaction. The energy loss of SENS is due to the energy released from the absorbed nucleon mass. Large mass SENS lose a small fraction of their kinetic energy and are able to traverse the earth without attenuation for all masses of our interest. Fig. 7 shows the energy loss of SENS with  $10^{-4} \leq \beta \leq 10^{-2}$  plotted versus radius for  $M_S = 1 \text{ TeV}$ .

Fig. 8 shows the mean free path  $\lambda$  of Q-balls type SENS versus Q-ball number  $Q$  for  $M_S = 1 \text{ TeV}$ .

## 4 Sensitivity to SECS of scintillators, streamer tubes and nuclear track detectors

In this section we discuss the response of liquid scintillators, of streamer tubes and of nuclear track detectors (in particular the MACRO CR39) to Q-balls, assuming that for  $10^{-4} < \beta < 10^{-2}$  the electric charge of SECS is constant.



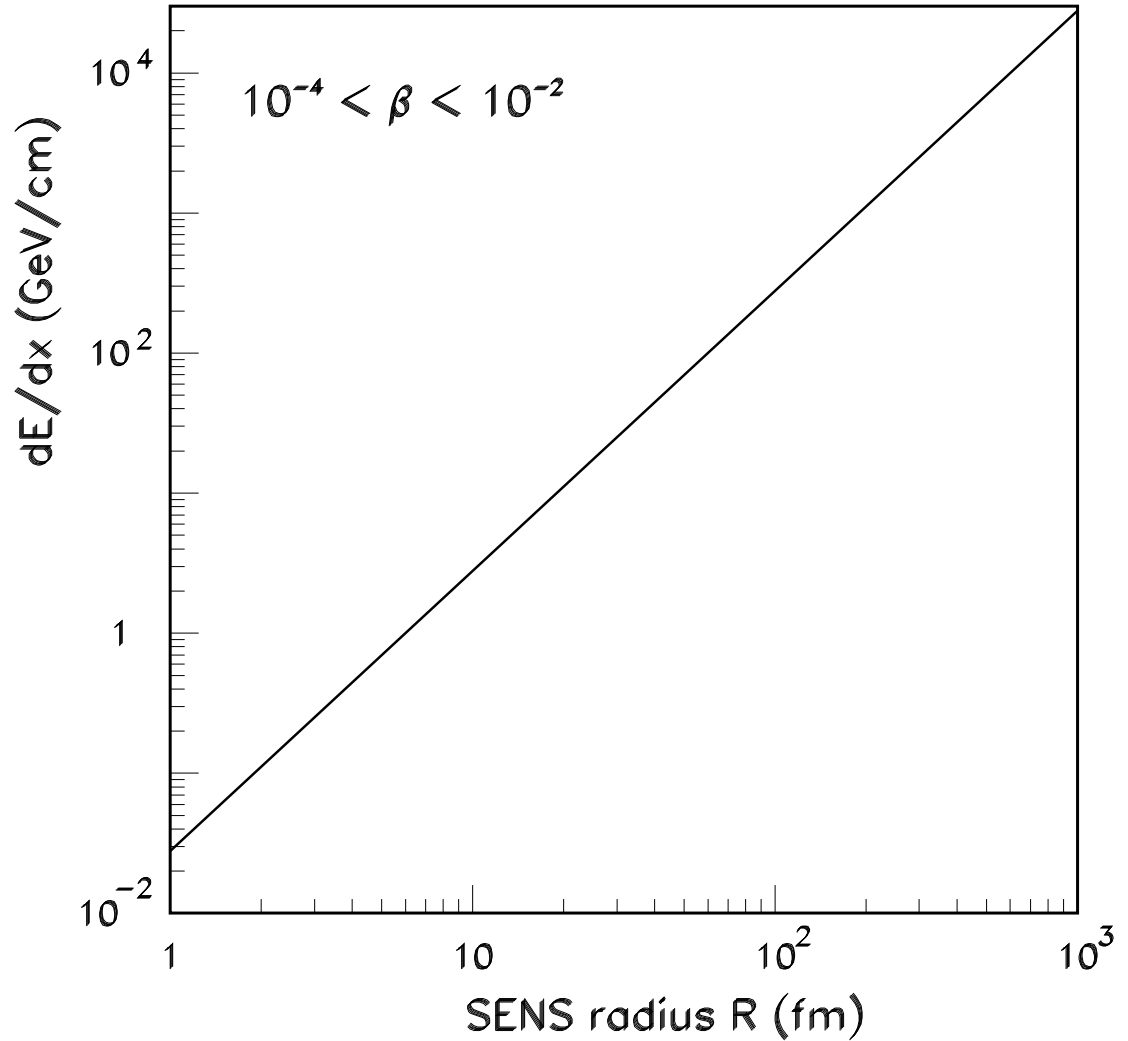


Figure 9: Energy loss of Q-ball type SENS with  $10^{-4} < \beta < 10^{-2}$  as function of the SENS radius  $R$  in a material, Eq. 18. This energy loss is in reality coming from the absorption of nucleons, see reactions (13),(14).

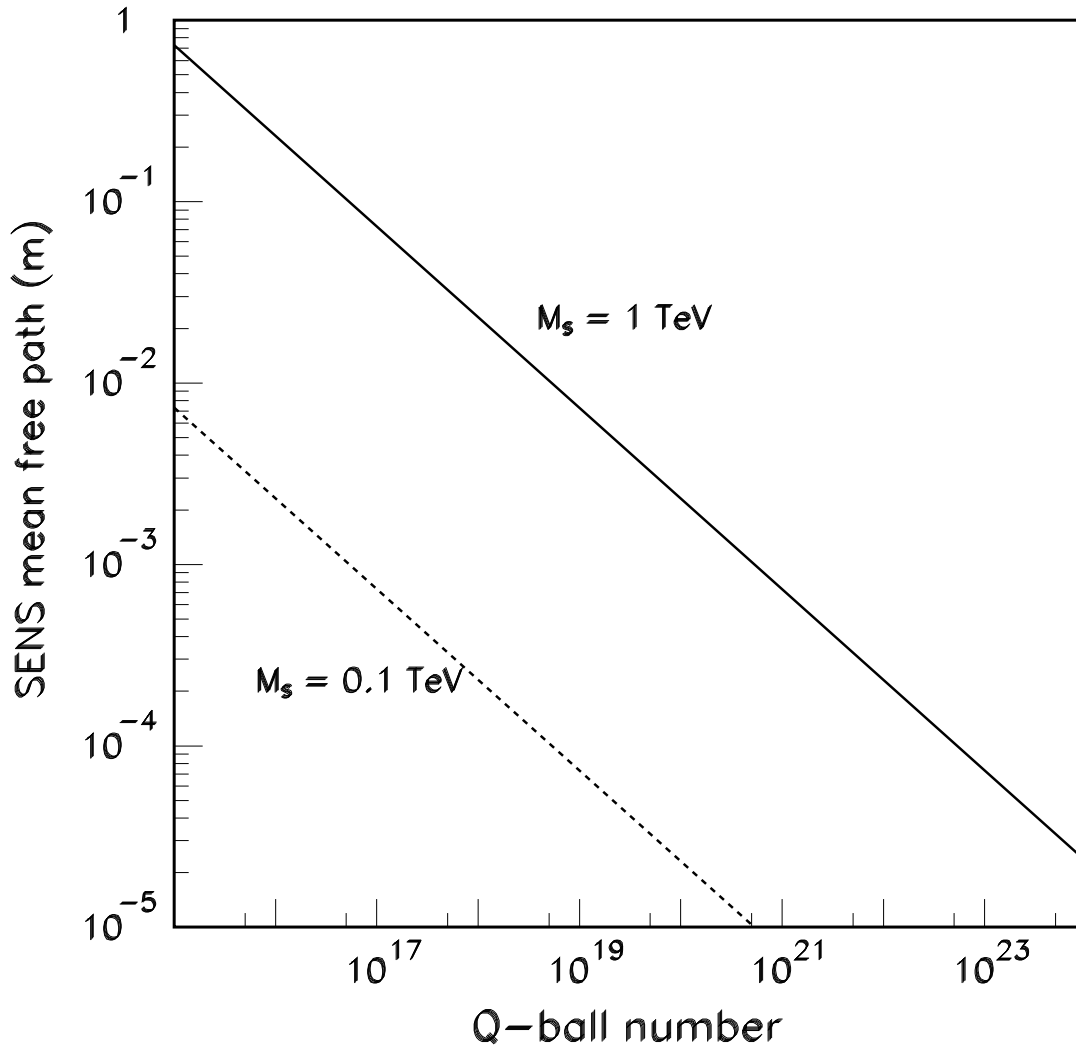


Figure 10: Mean free path of Q-ball type SENS for  $M_S = 1 \text{ TeV}$  and  $M_S = 0.1 \text{ TeV}$  as function of the Q-ball number, Eq. 17. The energy lost in each interaction is  $\sim 1 \text{ GeV}$  (absorption of one nucleon mass).

## 4.1 Light yield of Q-balls type SECS

The MACRO liquid scintillator has a density of 0.86 g/cm<sup>3</sup> and it is made of 96.4 % of mineral oil, 3.6 % of pseudocumene, 1.44 g/l of PPO, 1.44 mg/l of bis-MSB and 40 mg/l of antioxydant [6,7].

For SECS we distinguish two contributions to the light yield in scintillators: the primary light yield and the secondary light yield.

*The primary light yield:* it is due to the direct excitation (and ionization that occurs only for  $\beta > 10^{-3}$ ) produced by the SECS in the medium. The energy loss in the MACRO liquid scintillator is computed from the energy loss of protons in hydrogen and carbon [15]

$$\left(\frac{dE}{dx}\right)_{SECS} = \frac{1}{14} \left[ 2 \left(\frac{dE}{dx}\right)_H + 12 \left(\frac{dE}{dx}\right)_C \right] = SP = \frac{SL \times SH}{SL + SH} \quad (19)$$

where  $SP$  is the stopping power of SECS, which reduces to the lowest stopping power (SL) at low  $\beta$  and to the highest stopping power (SH) at high  $\beta$ . The stopping power coincides with the Bethe-Bloch formula for electric energy losses at relatively high velocities.

**1.** For electric charge  $q = 1e$  the energy loss of SECS in hydrogen and carbon is computed from [12] adding an exponential factor coming from the experimental data (see ref. [13]) on slow protons, see ref. [13].

**i)** For  $10^{-5} < \beta < 5 \times 10^{-3}$  we have the following formula

$$\left(\frac{dE}{dx}\right)_{SECS} = 1.3 \times 10^5 \beta \left[ 1 - \exp\left(-\frac{\beta}{7 \times 10^{-4}}\right)^2 \right] \frac{MeV}{cm} \quad (20)$$

**ii)** For  $5 \times 10^{-3} < \beta < 10^{-2}$  we used the following formula [13]

$$SP = SP_H + SP_C = \left(\frac{dE}{dx}\right)_{SECS} \quad (21)$$

where

$$SP_H = \frac{SL_H \times SH_H}{SL_H + SH_H} \quad (22)$$

$$SP_C = \frac{SL_C \times SH_C}{SL_C + SH_C} \quad (23)$$

and

$$SL = A_1 E^{0.45}, \quad SH = A_2 \operatorname{Ln} \left( 1 + \frac{A_3}{E} + A_4 E \right) \quad (24)$$

where ( $A_{i=1,4}$ ) are estimated in ref. [13] and  $E$  is the energy of a proton with velocity  $\beta$ .

**2.** For SECS with electric charge  $q = Z_1 e$  the energy losses for  $10^{-5} < \beta < 10^{-2}$  are given by [14]

$$\left( \frac{dE}{dx} \right)_{SECS} = \frac{8\pi e^2 a_0 \beta}{\alpha} \frac{Z_Q^{7/6} n_e}{(Z_Q^{2/3} + Z^{2/3})^{3/2}} \left[ 1 - \exp \left( -\frac{\beta}{7 \times 10^{-4}} \right)^2 \right] \quad (25)$$

where  $Z$  is the atomic number of the target atom,  $n_e$  the density of electrons and  $\alpha$  is the fine structure constant.

The primary light yield of SECS is given by [15]

$$\left( \frac{dL}{dx} \right)_{SECS} = A \left[ \frac{1}{1 + AB \frac{dE}{dx}} \right] \frac{dE}{dx} \quad (26)$$

where  $dE/dx$  is the total energy loss of SECS;  $A$  is a conversion constant of the energy losses in photons (light yield) and  $B$  is the parameter describing the saturation of the light yield; both parameters depend only on the velocity of SECS [12]. For example for the  $\beta$ -range,  $5 \times 10^{-5} < \beta < 10^{-3}$ ,  $A = 0.067$  and  $B = 0.66 \text{ cm/MeV}$ .

*The secondary light yield* arises from recoiling particles: we consider the elastic or quasi-elastic recoil of hydrogen and carbon nuclei. The light yield  $L_p$  from a hydrogen or carbon nucleus of given initial energy  $E$  is computed as

$$L_p(E) = \int_0^E \frac{dL}{dx}(\epsilon) S_{tot}^{-1} d\epsilon \quad (27)$$

where  $S_{tot}$  is the sum of electronic and nuclear energy losses,  $\epsilon$  is the excitation energy of the outer shell electrons. The nuclear energy losses are given in ref. [16]. The secondary light yield is then

$$\left( \frac{dL}{dx} \right)_{\text{secondary}} = N \int_0^{T_m} L_p(T) \frac{d\sigma}{dT} dT \quad (28)$$

where  $N$  is the number density of nuclei in the medium  $T_m$  is the maximum energy transferred and  $\frac{d\sigma}{dT}$  is the differential scattering cross section, given in ref. [17].

Fig. 9 shows the light yield of SECS in the MACRO liquid scintillator; for reference are also indicated the light yields of MMs with  $g = g_D$  and fast muons.

## 4.2 Energy losses of SECS in streamer tubes

The composition of the gas in the MACRO limited streamer tubes is 73% helium and 27% n-pentane, in volume [6]. The pressure is about one atmosphere and the resulting density is low (in comparison with the density of the other detectors):  $\rho_{gas} = 0.856 \text{ mg/cm}^3$ . The energy losses of MMs in the streamer tubes have been discussed in ref. [6,7].

The ionization energy losses of SECS in the MACRO streamer tubes for  $10^{-3} < \beta < 10^{-2}$  are computed with the same general procedure used for scintillators, using the density and the chemical composition of streamer tubes.

For  $q = 13e$  the ionization energy losses are calculated as in ref. [14] (we have omitted the exponential factor which takes into account the energy gap in organic scintillators).

The threshold for ionizing n-pentane occurs for  $\beta \geq 2 \times 10^{-3}$ .

Fig. 10 shows the ionization energy losses of SECS with electric charges  $q = 1$  and  $q = 13$  plotted versus  $\beta$ .

## 4.3 Restricted energy losses of SECS in the nuclear track detector CR39

The quantity of interest for nuclear track detectors is the Restricted Energy Loss (REL), that is, the energy deposited within  $\sim 100 \text{ \AA}$  diameter from the track.

The REL in CR39 has already been computed for MMs of  $g = g_D$  and  $g = 3g_D$  and for dyons with  $q = e$ ,  $g = g_D$  in ref. [18]. We have checked these calculations and extended them to other cases of interest, see ref. [6].

The chemical composition of CR39 is  $(C_{12}H_{18}O_7)_n$ , and the density is  $1.31 \text{ g/cm}^3$ . For the computation of the REL, only energy transfers to atoms

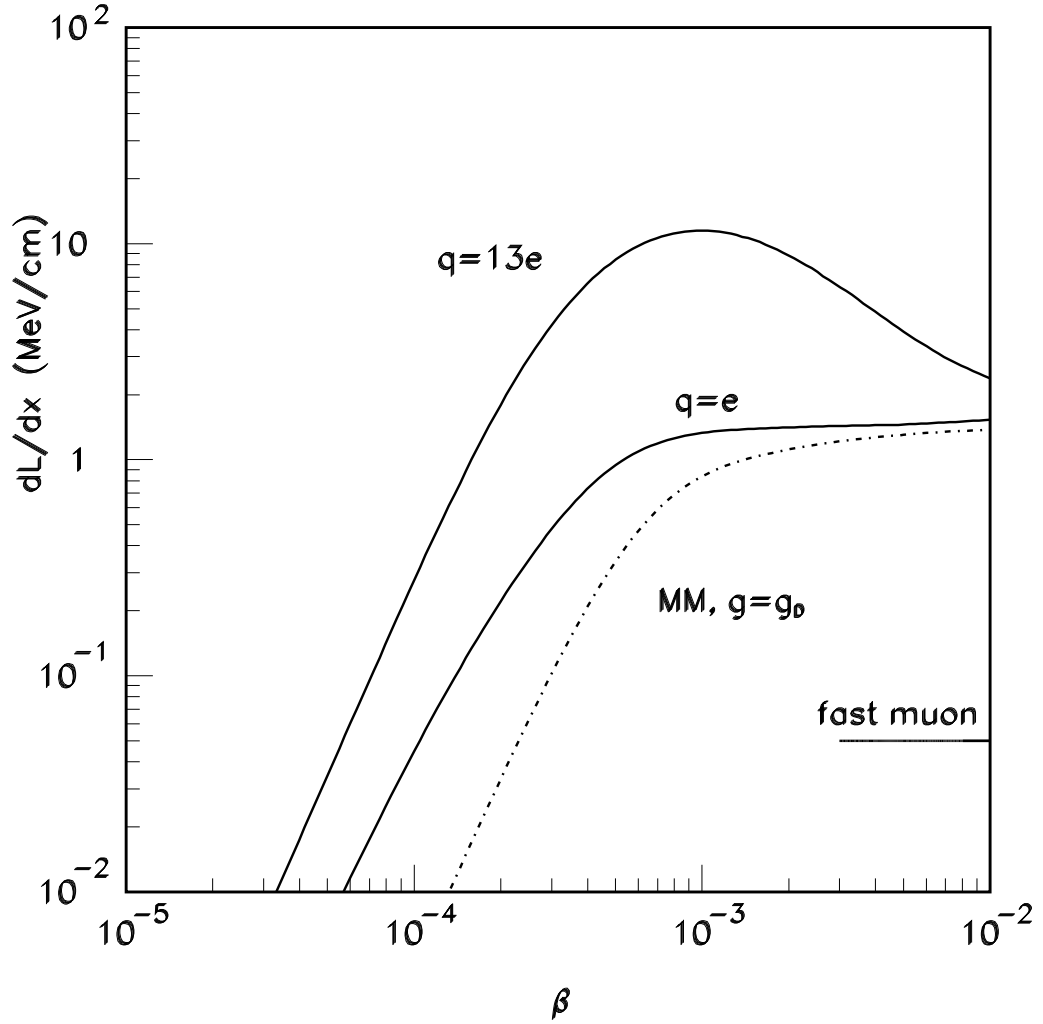


Figure 11: Light yield of SECS (solid lines) in the MACRO liquid scintillator as function of the SECS velocity;  $q$  is the net positive electric charge of the SECS. For comparison we give also the light yield of MMs with  $g = g_D$  (dotted-dashed line) and of fast muons. For  $2 \times 10^{-4} < \beta < 3 \times 10^{-3}$  there is no saturation of the light yield for  $q = 13e$  because it is the recoil nucleus which contributes to the light yield.

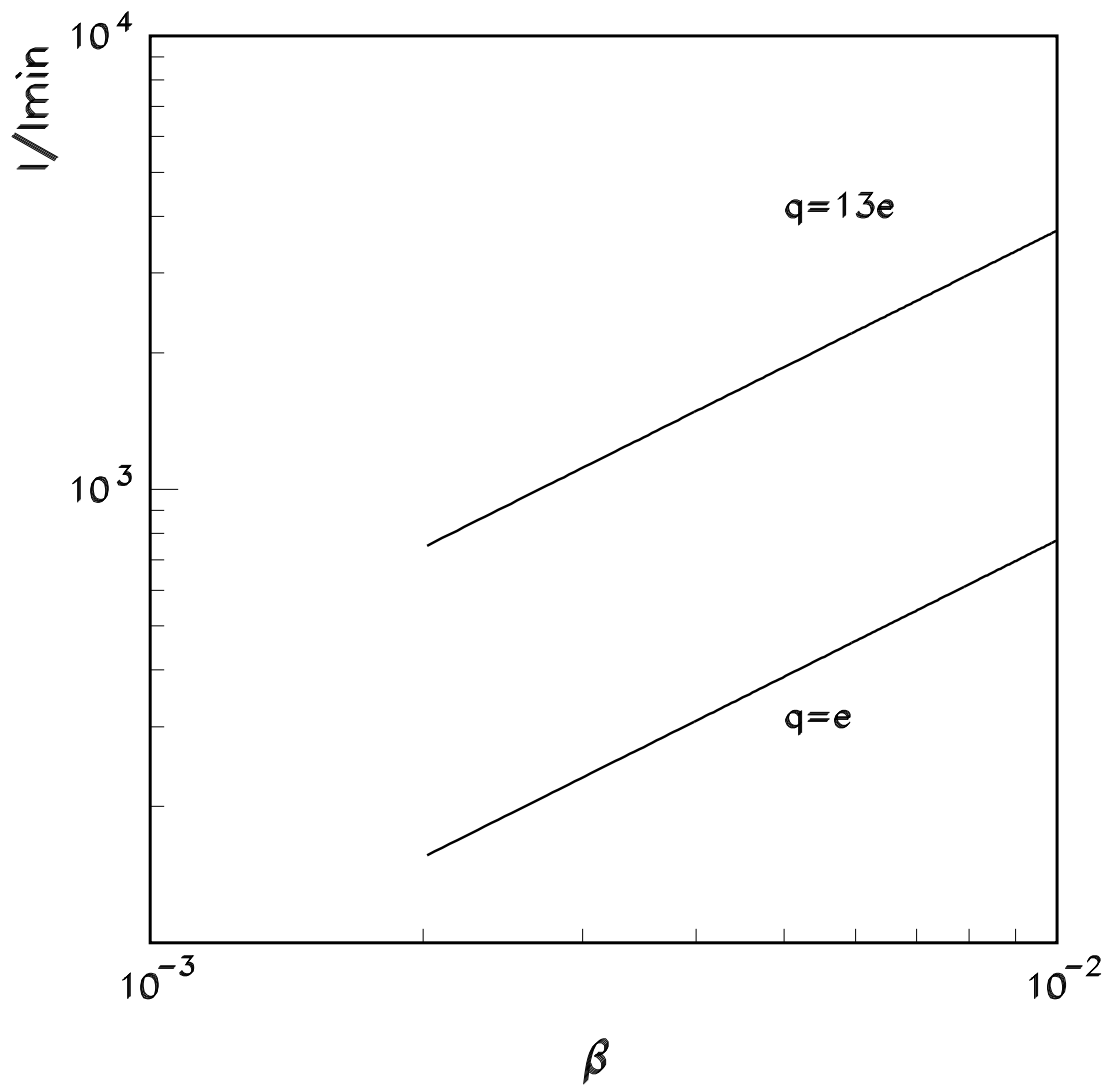


Figure 12: Ionization energy losses by SECS versus  $\beta$  in the limited streamer tubes, filled with 73% He and 27% n-pentane, and with density  $\rho_{gas} = 0.856 \text{ mg/cm}^3$ , relative to the ionization produced by a minimum ionizing particle,  $I_{min} = 2.2 \text{ MeVcm}^2\text{g}^{-1}$

larger than 12 eV are considered, because it is estimated that 12 eV are necessary to break the molecular bonds [15].

At *low velocities* ( $3 \times 10^{-5} < \beta < 10^{-2}$ ) there are two contributions to REL: the ionization and the atomic recoil contributions.

*The ionization contribution*, which becomes important only for  $\beta > 2 \times 10^{-3}$ , was computed with Ziegler's fit to the experimental data [12].

*The atomic recoil contribution*, which is important to REL for low  $\beta$  values was calculated using the interaction potential between an atom and a SECS [16]

$$V(r) = \frac{Z_Q Z e^2}{r} \phi(r) \quad (29)$$

where  $r$  is the distance between the core of SECS and the target atom,  $Z_Q e$  is the electric charge of the SECS core,  $Z$  is the atomic number of the target atom. The function  $\phi(r)$  is the screening function given by [16]

$$\phi(r) = \sum_1^3 C_i \exp\left[-\frac{b_i r}{a}\right] \quad (30)$$

where  $b_i$  and  $c_i$  are semiempirical constants given in Table 1 of ref. [16] and the coefficients  $C_i$  are restricted such that  $\sum_1^3 C_i = 1$ ,  $a$  is the screening length of Eq. [12].

Assuming the validity of the potential of Eq. 29, we calculate the relation between the scattering angle  $\theta$  and the impact parameter  $b$ . From this relation, the differential cross section  $\sigma(\theta)$  is obtained as [15]

$$\sigma(\theta) = -(db/d\theta) \cdot b / \sin \theta \quad (31)$$

The relation between the transferred kinetic energy  $K$  and the scattering angle  $\theta$  is given by the relation

$$K = 4E_{inc} \sin^2(\theta/2) \quad (32)$$

where  $E_{inc}$  is the energy of the atom relative to the SECS in the center of mass system. The restricted energy losses are finally obtained by integrating the transferred energies as

$$-\frac{dE}{dx} = N \int \sigma(K) dK \quad (33)$$



where  $N$  is the number density of atoms in the medium,  $\sigma(K)$  is the differential cross section as function of the transferred kinetic energy  $K$ .

Fig. 11 shows the computed REL in CR39 for SECS with  $q = 1e$  and  $q = 13e$  plotted versus  $\beta$ .

## 5 Conclusions

Supersymmetric generalizations of the Standard Model allow for stable non-topological solitons, called Q-balls, which may be considered as bags of squarks and sleptons and thus have non-zero baryon and lepton numbers; they have positive electric charge (SECS) or neutral (SENS) small masses [1-3]. The Q-ball could be produced in the Early Universe, could affect the nucleosynthesis of light elements, and could lead to a variety of other astrophysical and cosmological consequences.

In this paper, we computed the energy losses of Q-balls of type SENS and SECS. Using these energy losses and a rough model of the Earth's composition and density profiles, we have computed the angular acceptance of the an underground detector at the Gran Sasso Laboratory for Q-balls type SECS with  $v = 250 \text{ km/s}$  as function of the Q-ball mass  $M_Q$ . We have calculated the accessible region in the plane (mass, velocity) of SECS reaching the MACRO detector from above and from below.

We also presented an analysis of the energy deposited in the MACRO subdetectors: scintillators, streamer tubes and CR39 nuclear track detectors by SECS, in forms useful for their detection. In particular we computed the light yield in scintillators, the ionization in streamer tubes and the REL in nuclear track detectors.

The three MACRO subdetectors are sensitive to SECS with  $\beta \sim 10^{-3}$  and masses larger than  $10^{13} \text{ GeV}$  ( $10^{19} \text{ GeV}$ ) for SECS coming from above (below). A flux upper limit may be obtained from MACRO at the level of few times  $10^{-16} \text{ cm}^{-2}\text{s}^{-1}\text{sr}^{-1}$ .

SENS are more difficult to detect. MACRO scintillators could detect them, the streamer tubes have a limited efficiency and the CR39 detectors cannot see them.

**Acknowledgements:** We gratefully acknowledge the cooperation of many members of the MACRO collaboration, in particular of all the members of Bologna group. We thank A. Kusenko for stimulating discussions.

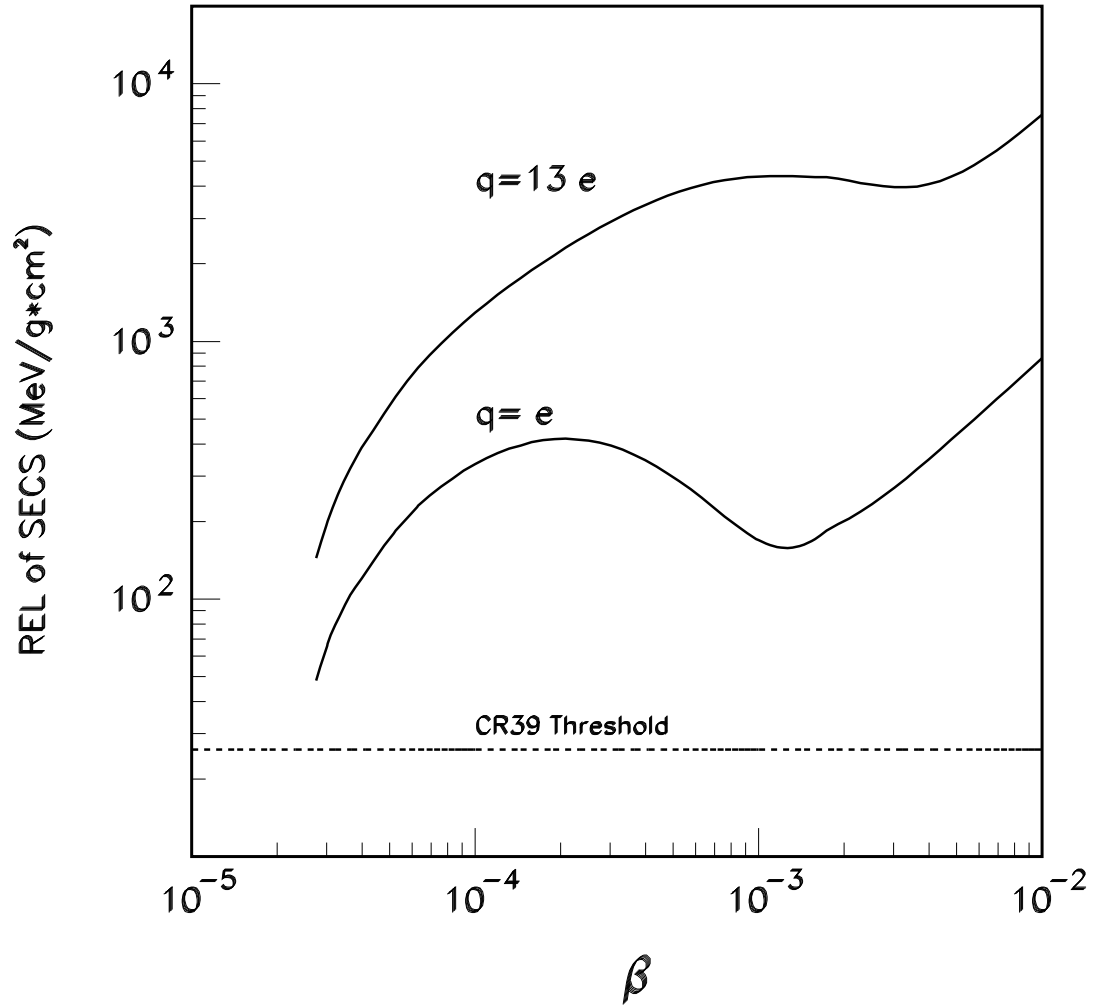


Figure 13: Restricted Energy Losses of SECS with charges  $e$  and  $13e$  as function of their velocity in the nuclear track detector CR39. The detection threshold for the MACRO CR39 is also shown, ref. [7].

## References

- [1] E. Witten, Phys. Rev. **D 30** (1984) 272;  
A. De Rujula and Glashow, Nature **312** (1984) 734;  
E. Farhi and R.L. Jaffe, Phys. Rev. **D 30** (1984) 2379.
- [2] T.D. Lee and Y. Pang, Phys. Rep. **221** (1992);  
R. Ruffini and A. Bonnazola, Phys. Rev. **187** (1969) 1767;  
J.D. Breit et al., Phys. Lett. **B140** (1984) 329;  
M. Colpi et al., Phys. Rev. Lett. **57** (1986) 2485.
- [3] S. Coleman, Nucl. Phys. **B 262** (1985) 293.
- [4] A. Kusenko, Phys. Lett. **B 405** (1997) 108; Phys. Lett. **B 404** (1997) 285; Phys. Lett. **B 406** (1997) 26.
- [5] A. Kusenko and M. Shaposhnikov, Phys. Lett. **B 417** (1998) 99;  
A. Kusenko, V.A. Kuzmin, M. Shaposhnikov and P.G. Tinyakov, Phys. Rev. Lett. **80** (1998) 3185.
- [6] G. Giacomelli, Riv. Nuovo **7** (1984);  
J. Derkaoui et al., Astropart. Phys. **9** (1998) 173.
- [7] S.P. Ahlen et al. MACRO Collaboration, Nucl. Instr. Meth. **A324** (1993) 337;  
M. Ambrosio et al. MACRO Collaboration, Phys. Lett. **406** (1997) 249;  
M. Ambrosio et al. MACRO Collaboration, “*Nuclearite Search with the MACRO Detector at Gran Sasso.*”, hep-ex/9904031, Eur. Phys. J. (in press).
- [8] J. Madsen, Phys. Lett. **B 435** (1998) 125;  
J. Madsen, Phys. Lett. **B 246** (1990) 135;  
A.V. Olinto, “*The Physics of Strange Matter*”, Proceedings of “*Relativistic Aspects of Nuclear Physics*”, Rio de Janeiro, Brazil (1991);  
J. Madsen, “*Physics and Astrophysics of Strange Quark Matter*”, astro-ph/9809032 (1998).
- [9] V.A. Rubakov, Rep. Prog. Phys. **51** (1988) 189.
- [10] M. Ouchrif, “*Q-balls in Underground Experiments*”, hep-ex/00002013.

- [11] T. Gherghetta, C. Kolda and S.P. Martin, Nucl. Phys. **B468** (1996) 37;  
G. Cleaver et al., “*Classification of flat directions in perturbative heterotic superstring vacua with anomalous  $U(1)$* ”, hep-th/9711178 (1997).
- [12] H. H. Andersen and J.F. Ziegler, “*Hydrogen stopping power and ranges in all elements*”, Pergamon Press (1977).
- [13] D. J. Ficenec et al., Phys. Rev. **D36** (1987) 311.
- [14] J. Lindhard and M. Scharff, Phys. Rev. **124** (1961) 28.
- [15] J. Derkaoui et al., Astropart. Phys. **10** (1999) 339;  
G. Giacomelli et al. “*Magnetic Monopole Bibliography*”, DFUB 9/98 (1998).
- [16] W. D. Wilson, L. G. Haggmark and J. P. Biersack, Phys. Rev. **B15** (1977) 2458.
- [17] J. Lindhard et al., K. Dan. Vidensk. Selsk. Mat.-Fys. Med. **33** (1963) No. 14.
- [18] T. W. Ruijgrok, J. A. Tjon and T. T. Wu, Phys. Lett. **129B** (1983) 209;  
S. Nakamura, Ph. D. Thesis, “*Search for supermassive relics by large area plastic track detectors*”, UT-ICEPP-88-04, University of Tokyo (1988).